International Journal of Mechatronics and Applied Mechanics
2026, Issue 25, Vol. II

QUASI-STATIC STATE-SPACE MODELING OF QUALITY AND TOOL WEAR IN CYLINDRICAL GRINDING

Roman Strelchuk[1][0000-0002-7221-031X], Andriy Fadieiev[1] [0009-0009-8436-5173], Serhii Nesterenko[1][0009-0006-1561-0487], Viktor Basov[1][0009-0007-2889-3946] and Paweł Zawadzki[2*][0000-0001-8153-8774]*
[1]National Technical University «Kharkiv Polytechnic Institute», Kharkiv, 61002, Ukraine
[2] Poznań University of Technology, Piotrowo 3, 61-138 Poznań, Poland
E-mail(s): Roman.Strelchuk@khpi.edu.ua, andrii.fadeiev@khpi.edu.ua, Serhii.Nesterenko@mit.khpi.edu.ua, Viktor.Basov@mit.khpi.edu.ua, pawel.zawadzki@put.poznan.pl

Abstract – This paper introduces a new quasi-static state-space model for estimating and forecasting part quality during in-process plunge cylindrical grinding. Drawing on an extensive survey of existing grinding models, the author identifies an underlying dynamic connection linking the grinding conditions, grinding power, surface roughness, and part dimensions – driven by both machine dynamics and progressive wheel wear. This relationship forms the basis for a nonlinear state-space formulation. Model parameters are calibrated using values drawn from published literature, and a series of simulations confirm that the model behaves in a physically realistic way. To date, this validation rests entirely on simulation using parameters drawn from the literature, not on original experimental data. Because certain outputs – such as the true part size – aren't always measurable in real manufacturing settings, the study also examines observability under several different output configurations, revealing how the choice of on-line sensors influences the model's ability to be observed. This framework introduces a novel method for inferring part qualities, including surface roughness and actual dimensions, by applying state estimation techniques to measurable outputs like grinding power. Furthermore, the model supports long-range forecasting of part quality across successive batch grinding cycles through simulation. The paper closes with a discussion of how this model could be applied to grinding process monitoring and control, along with an acknowledgment of the technical obstacles that remain to be addressed.

Keywords: Cylindrical grinding, State space model, Observability, Controllability, Wheel wear, Nonlinear dynamic systems.

1. Introduction

Advances in sensor technology, networking, and data storage have led to an explosion of data collected on modern factory floors. Comprehensive surveys of sensor applications in machining and grinding are available elsewhere [1, 2]. As this trend continues, the competitiveness of manufacturers will increasingly hinge on their ability to convert raw sensor data into actionable insight. Yet despite the sheer volume of information now available, both researchers and practitioners recognize that this data remains significantly underused. A central obstacle is the mismatch in timing between process-variable measurements and product-quality measurements. In grinding operations, for instance, sensors routinely capture process variables in real time – power draw, cutting forces, vibration, and acoustic emission – whereas critical quality metrics like surface finish, subsurface integrity, and roundness typically can only be assessed after the fact, off-line.

Because part quality is so difficult to measure during processing, considerable research effort has gone into inferring these qualities indirectly from sensor data, largely through statistical methods or neural-network-based signal processing [1, 2]. Comparable strategies have also been used to indirectly track tool wear. Notably, Danai and Ulsoy introduced a dynamic-state-model approach to estimate tool wear in turning operations [3], treating wear as a hidden state driven by machining conditions, with cutting force as the observable output; standard observer or estimation techniques could then be applied to infer wear in real time. This method offered the benefit of naturally combining information from multiple sensors and integrating directly into closed-loop control schemes. The approach was later generalized to broader classes of nonlinear systems using

dx.doi.org/10.17683/ijomam/issue25/v2.22

radial basis function networks [4]. Building on this success in tool-wear monitoring, the current study proposes an analogous dynamic-state framework, applied instead to the estimation of ground-part quality.

Grinding process control has also advanced substantially in the past decade, though it continues to pose challenges due to the process's nonlinear, stochastic, and time-varying nature. Many existing control strategies address only a single variable or a pair of variables – for example, grinding force [5] or dimensional accuracy [6, 7] – rather than tackling quality holistically. A more comprehensive framework spanning multiple part-quality metrics was developed by Danai and Malkin [8, 9], though its design is tightly coupled to particular experimental setups. Because their algorithm was built around minimizing cycle time specifically, it is unclear how readily it could be adapted to alternative goals, such as cost reduction. Moreover, none of these prior control schemes incorporate a systematic mechanism for updating model parameters based on off-line quality measurements taken after processing.

By contrast, the semiconductor industry has embraced run-to-run control as a standard strategy for batch process management [10]. Under this paradigm, process recipes are adjusted between runs using quality data gathered from prior batches – an approach that has become foundational to processes like chemical-mechanical planarization (CMP) [11]. While run-to-run control has not been formally adopted in grinding, related post-process adjustment strategies have appeared in a small number of studies [12, 13]. Comparing conventional real-time grinding control with CMP's run-to-run methodology suggests a promising direction: grinding control stands to benefit from more deliberately combining real-time sensor data with periodic off-line quality checks, much as CMP does.

This paper proposes exactly such an integration – linking in-process sensor measurements to off-line quality assessments through a unified quasi-static state-space model. A key strength of this approach is that it naturally fuses signals from multiple sensors, improving the robustness of quality estimates. Unlike prior signal-processing or probabilistic estimation methods, this state-space formulation supports not only estimating current part quality but also forecasting quality outcomes several cycles into the future. This capability opens the door to optimized grinding control strategies applicable to a wide range of objectives and constraints.

The remainder of the paper is organized as follows: Section 2 derives the proposed state-space model from established grinding relationships in the literature and presents simulation results for both single and repeated grinding cycles. Section 3 explores potential monitoring and control applications, including an analysis of the model's observability and controllability.

2. Method for Modeling the Spatial State of a Process

This section develops a state-space representation of the plunge cylindrical grinding process, synthesizing relationships established in prior literature. Although the derivation here focuses on plunge cylindrical grinding, a comparable methodology could be extended to other grinding configurations, such as surface grinding. Figure 1 illustrates the grinding system and identifies the principal process variables considered in this study.

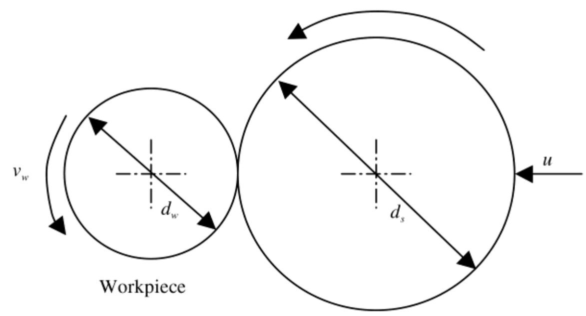

Figure 1: Configuration of a cylindrical grinding process.

Under the assumption that wheel speed remains constant and that changes in wheel diameter from wear are negligible within a single grinding cycle, the relationship between the commanded infeed rate, u (*mm/s*), and the actual infeed rate, v (*mm/s*), can be modeled as a first-order dynamic system [1, 14]:

$$u - v = \tau \frac{dv}{dt}, \tag{1}$$

where τ is a time constant (*s*) governed by the combined stiffness of the machine, wheel, and workpiece, as well as wheel dullness and wheel speed:

$$\tau = \frac{D\pi d_w b_s}{k v_s}, \tag{2}$$

where D denotes wheel dullness, d_w is the workpiece diameter (*mm*), b_s is the wheel width (*mm*), k is system stiffness (*N/mm*), and v_s is wheel speed (*m/s*). Wheel dullness increases monotonically with the accumulated metal removed per unit wheel width since the last dressing, $V_w^{'}$ (mm^3/mm):

$$D = D_0 + D_1 V_w^{'\delta}, \tag{3}$$

where $\dot{V}_w^{'} = \pi d_w v$, and D_1 and δ are constants; D_0 depends on dressing parameters such as dressing lead and depth. For consistency with the notation used in Table 1, these same wear-law constants are denoted s_0, s_1, and δ there; the two symbol sets refer to identical parameters and are used interchangeably between the text and the table. Grinding power, P (W), can be approximated for moderate wheel speeds as a linear function of the metal removal rate:

$$P = \mu D \pi d_w b_s v, \tag{4}$$

where μ is the friction coefficient, and P reflects power in excess of the threshold grinding power. Substituting Equation (3) into Equation (4) yields an expression for grinding power as a function of v and $V_w^{'}$:

$$P = K_s (s_0 + s_1 V_w^{'\delta}) \mathrm{v}, \tag{5}$$

with $K_s = k\mu,\ s_0 = D_0 \pi d_w b_s / k,\ s_1 = D_1 \pi d_w b_s / k$.
Surface roughness, R_a (μm), evolves over time according to the following empirical relation reported in the literature [14]:

$$R_a = \left[R_g + \left(R_o^* - R_g \right) \exp\left(-\frac{V_w^{'}}{V_0^{'}} \right) \right] \left(\frac{\pi d_w v}{v_s} \right)^{\gamma}, \tag{6}$$

Equations (1)–(6) can be combined into a state-space form by treating $V_w^{'}$ and v as state variables x_1 and x_1, respectively, and assuming $\dot{v}_s = 0$ within a single grinding cycle. In this formulation, the command infeed rate u and wheel speed v_s serve as system inputs u_1 and u_2, while grinding power P and surface roughness R_a constitute the system outputs y_1 and y_2:

$$\begin{bmatrix} \dot{x}_1 \\ \dot{x}_2 \end{bmatrix} = \begin{bmatrix} \pi d_w x_2 \\ \dfrac{u_2 (u_1 - x_2)}{s_0 + s_1 x_1^{\delta}} \end{bmatrix}, \tag{7}$$

$$\begin{bmatrix} y_1 \\ y_2 \end{bmatrix} = \begin{bmatrix} K_s (s_0 + s_1 x_1^{\delta}) x_2 \\ \left[R_g + \left(R_o^* - R_g \right) \exp\left(-\dfrac{x_1}{V_0^{'}} \right) \right] \left(\dfrac{\pi l_w x_2}{u_2} \right)^{\gamma} \end{bmatrix}. \tag{8}$$

Beyond predicting grinding power and roughness, the framework can be extended to additional outputs. The cumulative reduction in part diameter since dressing, D_w (mm), follows directly from the state variable x_1:

$$D_w = \frac{2 x_1}{\pi d_w}. \tag{9}$$

Out-of-roundness, r (μm), is known to vary linearly with the working engagement [9], and can be expressed in terms of state variable x_1 and the work speed v_w (m/s):

$$r = r_0 \frac{\pi d_w x_2}{v_w} + r_m, \tag{10}$$

where r_0 and r_m are constants.

While radial wheel wear during a single cycle is typically negligible, its cumulative effect across a batch of cycles becomes significant. The grinding ratio (G-ratio), defined as the volumetric ratio of metal removed to wheel material consumed, is expressed as:

$$G = \frac{d_w v}{d_{s0} w}, \tag{11}$$

where d_{s0} is the wheel diameter immediately after dressing, and w is the radial wheel wear rate (mm/s). A widely cited empirical model for the G-ratio [15] is:

$$G = G_1 \left(\frac{\pi d_w v}{v_s} \right)^{-g}, \tag{12}$$

where G_1 and g are constants. Combining Equations (11) and (12) with the identity $\dot{d} = -2w$ yields an expression for the time evolution of wheel diameter d_s (mm):

$$\dot{d} = -\frac{2\pi^g d_w^{1+g}}{d_{s0} G_1} u_2^{-g} x_2^{1+g}. \tag{13}$$

Taken together, the complete quasi-static state-space model of the cylindrical grinding process can be expressed compactly as:

$$\dot{x} = f(x,u), \tag{14}$$

$$y = h(x,u). \tag{15}$$

where $x = (x_1, x_2, x_3)^T = (Vw', v, d_s)^T \in \Re^3$,
$u = (u_1, u_2)^T = (u, v_s)^T \in \Re^2$ and
$y = (y_1, y_2, y_3, y_4, y_5)^T = = (P, R_a, D_w, r, d_s)^T \in \Re^5$.
The two nonlinear functions in equations (14) and (15) are given as:

$$f(x,u) = \begin{bmatrix} \pi d_w x_2 \\ \dfrac{u_2(u_1 - x_2)}{s_0 + s_1 x_1^{\delta}} \\ -\dfrac{2\pi^g d_w^{1+g}}{d_{s0} G_1} u_2^{-g} x_2^{1+g} \end{bmatrix}, \tag{16}$$

$$h(x,u) = \begin{bmatrix} K_s (s_0 + s_1 x_1^{\delta}) x_2 \\ \left[R_g + (R_o^* - R_g) exp\left(-\frac{x_1}{V_0^{'}} \right) \right] \left(\frac{\pi d_w x_2}{u_2} \right)^{\gamma} \\ \frac{2x_1}{\pi d_w} \\ r_0 \frac{\pi d_w x_2}{v_w} + r_m \\ x_3 \end{bmatrix}. \tag{17}$$

Figure 2 depicts the overall architecture linking system inputs, states, and outputs. As shown, grinding power is measurable on-line whenever a power meter is installed, while surface roughness and out-of-roundness are typically only obtainable off-line; part size may be sampled either on-line or off-line depending on gauge availability. In this way, the proposed model unifies on-line and off-line measurements within a single, coherent framework.

When on-line signals – such as power or part size – are available, a state estimation technique like the extended Kalman filter can be applied to infer the internal states, from which roughness and out-of-roundness can subsequently be computed via the output equation. Applications of this framework to grinding process monitoring and control are discussed further in later sections.

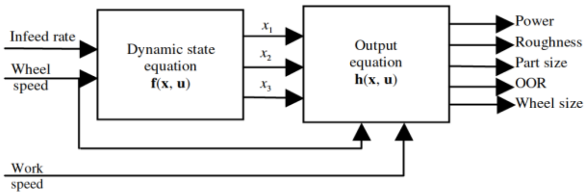

Figure 2: Proposed state space model of a grinding process

The proposed model was applied to simulate an internal cylindrical plunge grinding process. Table 1 summarizes the parameter values used in Equations (16) and (17), compiled from several literature sources [16–18].

Table 1. Model parameters used in simulation

d_w (mm)	d_{s0} (mm)	s_0	s_1	K_s (N/mm)	δ	γ
72	52	49.2	0.07	2380	1	0.35
R_g	R_0	V_0' (mm^3/mm)	r_m	r_0	G_1	g
2.75	7.2	300	2.35	1	12	0.88

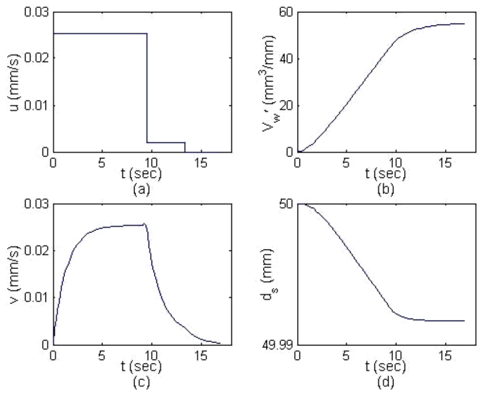

Figure 3: Command infeed rate and the 3 state variables over a simulated grinding cycle: (a) Command infeed rate, u (mm/s) (b) Accumulated metal removal per unit wheel width after dressing, V_w' (mm^3/mm)
(c) Actual infeed rate, v (mm/s)
(d) Wheel diameter, d_s (mm)

Simulation results for a single grinding cycle appear in Figure 3. Wheel speed and work speed were held constant at 35 m/s and 0.53 m/s, respectively, while the commanded infeed rate followed a three-stage schedule corresponding to roughing, finishing, and spark-out (Figure 3a). The nonlinear state equation (16) was solved using a standard Runge–Kutta method in MATLAB, with initial condition x_0=(0,0,50). Figures 3b–d trace the evolution of the three state variables. Comparing Figures 3a and 3c reveals the time lag introduced by machine dynamics (Equation 1); the effect of wheel dulling, however, is not perceptible within a single cycle. Figure 3d further shows that most wheel wear accumulates during the roughing stage.

Figure 4 presents the first four output variables corresponding to the states in Figure 3, while the fifth output tracks the same wheel diameter shown in Figure 3d, per Equation (17). Note that the grinding power in Figure 3a reflects power net of the threshold value; in practice, measured spindle power would not approach zero during spark-out. Figures 4b–d illustrate the corresponding evolution of surface roughness, part diameter, and out-of-roundness across the cycle.

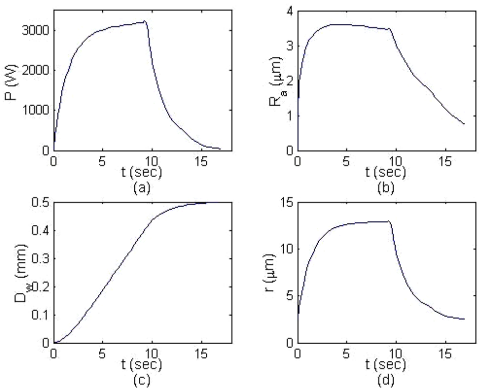

Figure 4: Change of four output variables over a simulated grinding cycle: (a) Grinding power, P (W)
(b) Surface roughness, R_a (µm)(c) Accumulated reduction in diameter of the part after dressing, D_w (mm)
(d) Out of roundness, r (µm)

Beyond single-cycle simulation, the model was extended to represent multiple sequential grinding cycles. At the start of each new cycle, the initial state vector is set using the final state of the preceding cycle: both the accumulated metal removal per unit wheel width, V_w', and wheel diameter, d_s, carry over from the prior cycle, while the actual infeed rate, *v*, resets to zero. This process repeats until the wheel is redressed, at which point V_w' and d_s are reset.

Figure 5 depicts this simulation horizon schematically.

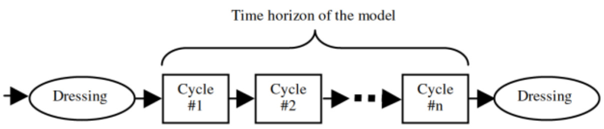

Figure 5: Simulation horizon of the proposed model.

Figure 6 and 7 present results for ten consecutive grinding cycles following a single dressing operation, using the same parameters and infeed schedule as the single-cycle case. The cumulative effect of wheel dulling on grinding power and surface roughness becomes clearly visible in Figure 6.

Figures 7a–c plot end-of-cycle part quality metrics against cycle number. Although Figure 6c might suggest a steadily declining surface roughness trend across cycles, the end-of-cycle values in Figure 7a show no such consistent pattern.

This apparent discrepancy is explained by the end-of-cycle infeed rate shown in Figure 7d: as wheel dulling progresses, the time constant in Equation (1) increases per Equations (2) and (3), and with spark-out duration fixed, this leads to a rising actual infeed rate at cycle's end.

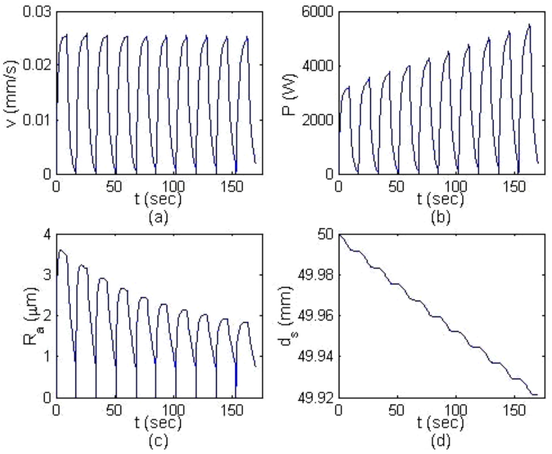

Figure 6: Change of 4 variables over 10 consecutive grinding cycles in simulation: (a) Actual infeed rate, v (mm/s) (b) Grinding power, P (W) (c) Surface roughness, R_a (µm) (d) Wheel diameter, d_s (mm).

Because increased dulling and rising infeed rate exert opposing influences on surface roughness, their interaction produces the fluctuations observed in Figure 7a.

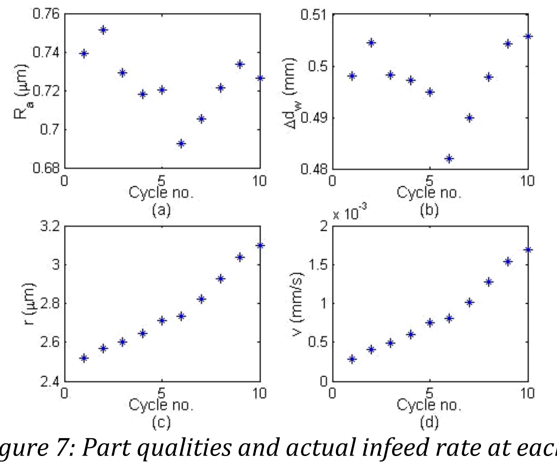

Figure 7: Part qualities and actual infeed rate at each end of 10 consecutive grinding cycles: (a) Surface roughness, R_a (µm) (b) Removed diameter of each part, _d_w (mm) (c) Out of roundness, r (µm) (d) Actual infeed rate at the end of each cycle, v (mm/s).

The considerable variability in part quality shown in Figure 7 – despite a fixed grinding schedule – underscores the need for more advanced control and optimization strategies in batch grinding production. Because increased dulling and rising infeed rate exert opposing influences on surface roughness, their interaction produces the fluctuations observed in Figure 7a. The considerable variability in part quality shown in Figure 7 – despite a fixed grinding schedule – underscores the need for more advanced control and optimization strategies in batch grinding production.

This simulation study demonstrates that the proposed model readily accommodates both single-cycle and multi-cycle analysis, capturing the intricate interdependencies among grinding variables within a unified state-space framework. The results confirm that the model behaves in a physically plausible manner. Future work should include experimental validation of the model under realistic conditions involving measurement noise and process disturbances.

3. Results and Discussions

The preceding section demonstrated that the proposed model provides a unified framework for simulating and analyzing the grinding process. However, its greater practical value lies in enabling the monitoring and control of grinding operations.

Given a specific set of measured outputs – such as grinding power – an adaptive filter or observer can, in principle, be constructed from the proposed model to estimate the internal states and unmeasured outputs, including various part-quality metrics, in real time. Figure 8 presents a schematic of this observer structure, where a hat symbol denotes an estimated variable or quantity.

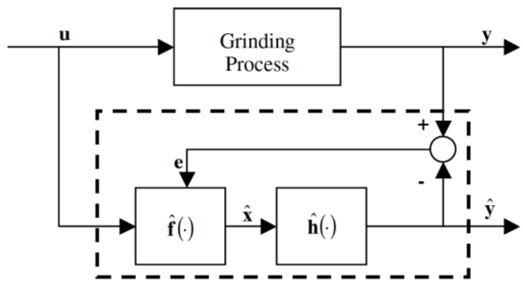

Figure 8: Schematic diagram of the observer for in-process estimation of part qualities.

As shown, the discrepancy between the estimated and measured outputs is fed back into the filter to refine the estimate of the state vector, $\hat{x}$. The design and implementation of such an optimal filter is left for future work. As established previously, the model also supports forecasting part quality over subsequent grinding cycles given a specified schedule of grinding conditions.

This capability suggests the feasibility of a model-based optimal control scheme, in which the grinding schedule is continually re-optimized using an updated process model at each sampling interval. Developing such a control strategy for a general class of objectives and constraints is left to future research. To assess the model's suitability for these purposes, its observability and controllability were examined. Although linearization is not necessarily the most rigorous approach for analyzing a nonlinear system, it offers a computationally efficient means of approximating these properties. The model was linearized about four operating points selected at random from the ten-cycle simulation results shown in Figure 6. Table 2 summarizes the observability rank obtained for three different combinations of measured outputs; a rank of 3 indicates that all three state variables are observable, while a lower rank indicates that only a subset can be estimated.

Table 2. Rank of the observability matrix based on 3 different sets of measured outputs at 4 different operating points

Operating point (x_1, x_2, x_3, u_1, u_2)	Observability rank		
	P	(P, D_w)	(P, D_w, d_s)
(216, 0.0076, 49.97, 0.002, 37)	2	2	3
(55, 0.0006, 49.99, 0, 37)	2	2	3
(110, 0.0012, 49.98, 0.0254, 37)	2	2	3
(381, 0.0001, 49.94, 0.0254, 37)	2	2	3

As the second column of Table 2 indicates, monitoring grinding power alone consistently yields a rank of 2, regardless of operating point–meaning two of the three states can be recovered from power measurements alone. Inspection of Equations (16) and (17) confirms that these two observable states correspond to $V_w^{'}$ and *v*. The third column shows that adding a size gauge to monitor D_w does not improve observability beyond this rank; full observability (rank 3) is achieved only when wheel diameter, d_s, is directly measured. Nonetheless, Equation (17) indicates that P, R_a, D_w, and r can all still be estimated from and v alone. This suggests that, at least in theory, surface roughness, part size, and out-of-roundness can be inferred solely from grinding power measurements. In practice, however, supplementing power monitoring with direct measurement of D_w via a size gauge would enhance the robustness of quality estimation. Wheel diameter measurement, d_s – though typically performed off-line–appears to be a particularly valuable source of process information. Table 3 reports the results of the corresponding controllability analysis, based on the same linearized models used above.

Table 3. Rank of the controllability matrix based on 3 different sets of manipulated inputs at 4 different operating points

Operating point (x_1, x_2, x_3, u_1, u_2)	Observability rank		
	u	v_s	(u, v_s)
(216, 0.0076, 49.97, 0.002, 37)	2	3	3
(55, 0.0006, 49.99, 0, 37)	2	3	3
(110, 0.0012, 49.98, 0.0254, 37)	2	3	3
(381, 0.0001, 49.94, 0.0254, 37)	2	3	3

As shown in the second column, manipulating the command infeed rate alone is insufficient to independently control all three state variables. Full controllability (rank 3) is achieved only when wheel speed is also manipulated, as demonstrated in the third and fourth columns. Although the model derivation assumed a fixed wheel speed within each grinding cycle, these results indicate that allowing wheel speed to vary would be essential for achieving more flexible and complete control over the grinding process. It is worth noting that the four linearization points used in Tables 2 and 3 were drawn at random from a single ten-cycle simulation run, and the observability and controllability ranks were identical at all four points tested. While this consistency is encouraging, it should not be read as a guarantee that the ranks hold uniformly across the process's full operating range: points drawn from a different simulation run, a different infeed schedule, or regions near the boundaries of the state space (e.g., very low or very high accumulated wear) could in principle yield different ranks. A more systematic sensitivity analysis, sweeping the linearization point across a fine grid of the reachable state space rather than relying on four randomly chosen samples, would be needed to establish how robust these observability and controllability findings are, and is left for future work.

4. Conclusions

This paper has introduced a novel, control-oriented state-space model for the cylindrical plunge grinding process, developed by synthesizing established relationships from the grinding literature into a unified nonlinear dynamic framework. Rather than treating grinding power, surface roughness, part size, and out-of-roundness as independent quantities to be modeled separately, the proposed formulation captures the underlying dynamic coupling among these variables, mediated by machine dynamics and progressive wheel wear.

Through simulation, the model was shown to reproduce physically plausible behavior across both single grinding cycles and extended sequences of batch cycles, capturing phenomena such as the time lag introduced by machine dynamics, the gradual influence of wheel dulling on process outputs, and the resulting variability in part quality across a production batch. These results confirm that the model provides a coherent and internally consistent representation of the grinding process, bridging the gap between real-time sensor signals and quality characteristics that are typically only assessable off-line.

Because the model is expressed as a standard nonlinear state-space equation, it lends itself naturally to state estimation techniques such as the extended Kalman filter, enabling in-process inference of part qualities that would otherwise require destructive or delayed ex-situ measurement. The observability analysis presented in this work indicates that, in principle, surface roughness, part size, and out-of-roundness can all be estimated from grinding power measurements alone, though supplementing this with direct wheel-diameter monitoring would likely improve estimation robustness in practice. Similarly, the controllability analysis revealed that flexible, comprehensive control of the grinding process requires manipulation of both infeed rate and wheel speed, rather than infeed rate alone.

Beyond estimation, the model's capacity for long-term prediction across successive grinding cycles suggests significant potential for model-based optimal control in batch grinding operations. All results reported here are based on simulation using parameters compiled from the literature, and the model has not yet been validated against original experimental data. Future research should prioritize experimental validation of the model under realistic conditions involving sensor noise and process disturbances, as well as the design and implementation of practical observer and control algorithms building on the theoretical foundation established here.

Acknowledgments

The general approach has been partially developed within the research project “Formation and transformation of periodic nanocarbon-containing structures on metal surfaces with short-pulse laser, microwave, and plasma methods” (State reg. no. 0124U000481) supported by the Ministry of Education and Science of Ukraine.

References

[1] Pimenov, D. Yu., Ribeiro da Silva, L. R., Kuntoğlu, M., Abrão, B. S., dos Santos Paes, L. E., & Linul, E. (2025). Review of advanced sensor system applications in grinding operations. *Journal of Advanced Research*, *77*, 371–405. https://doi.org/10.1016/j.jare.2025.01.013

[2] Kishore, K., Sinha, M. K., Singh, A., Archana, Gupta, M. K., & Korkmaz, M. E. (2022). A comprehensive review on the grinding process: Advancements, applications and challenges. *Proceedings of the Institution of Mechanical Engineers, Part C: Journal of Mechanical Engineering Science*, *236*(22), 10923–10952.https://doi.org/10.1177/09544062221110782

[3] Duan, J., Cao, G., Ma, G., Yu, Z., & Shao, C. (2024). Research on On-Line Monitoring of Grinding Wheel Wear Based on Multi-Sensor Fusion. *Sensors*, *24*(18), 5888. https://doi.org/10.3390/s24185888

[4] Christiand, Kiswanto, G., Baskoro, A. S., Hasymi, Z., & Ko, T. J. (2024). Tool Wear Monitoring in Micro-Milling Based on Digital Twin Technology with an Extended Kalman Filter. *Journal of Manufacturing and Materials Processing*, *8*(3), 108. https://doi.org/10.3390/jmmp8030108

[5] Novikov, F. (2025). High-quality diamond grinding of products made of materials of increased hardness. *IOP Conference Series: Earth and Environmental Science*, *1491*(1), 012031. https://doi.org/10.1088/1755-1315/1491/1/012031

[6] Dichev, D., Zhelezarov, I., Karadzhov, T., Georgiev, B., Kupriyanov, O., & Dicheva, R. (2025). Improving Accuracy in Dynamic Systems through Adaptive Identification of Model Errors within the Kalman Filter Structure. *Int. Sci. Symp. Metrol. Metrol. Assur., MMA*, (2025). https://doi.org/10.1109/MMA67107.2025.11311326

[7] Hashimoto, F., & Iwashita, H. (2020). The Effect of Grinding Wheel Contact Stiffness on Plunge Grinding Cycle. *Inventions*, *5*(4), 62. https://doi.org/10.3390/inventions5040062

[8] Hashimoto, F. (2020). The Design of an Infeed Cylindrical Grinding Cycle. *Inventions*, *5*(3), 46. https://doi.org/10.3390/inventions5030046

[9] Strelchuk, R., & Shelkovyi, O. (2022). Determination of the Distance Between Grains During Electrical Discharge Grinding with Changing Polarity of Electrodes. *Lect. Notes Mech. Eng.*, 209–218. https://doi.org/10.1007/978-3-030-91327-4_21

[10] Roman, S., Mittsel, M., & Stanciu, A. (2025). X-RAY DIFFRACTION STUDY OF RESIDUAL STRESSES IN WC-CO INDUCED BY POLARITY-SWITCHING ELECTRICAL DISCHARGE GRINDING. *International Journal of Mechatronics and Applied Mechanics*, *1*(20), 153–159. https://doi.org/10.17683/ijomam/issue20.15

[11] Lajmert, P., Sikora, M., & Ostrowski, D. (2018). A dynamic model of cylindrical plunge grinding process for chatter phenomena investigation. *MATEC Web of Conferences*, *148*, 09004. https://doi.org/10.1051/matecconf/201814809004

[12] Guo, W., Wu, C., Ding, Z., & Zhou, Q. (2021). Prediction of surface roughness based on a hybrid feature selection method and long short-term memory network in grinding. *The International Journal of Advanced Manufacturing Technology*, *112*(9), 2853–2871. https://doi.org/10.1007/s00170-020-06523-z

[13] Wang, D., Han, C., Wang, L., Li, X., Cai, E., & Zhang, P. (2023). Surface roughness prediction of large shaft grinding via attentional CNN-LSTM fusing multiple process signals. *The International*

Journal of Advanced Manufacturing Technology, *126*(11), 4925–4936. https://doi.org/10.1007/s00170-023-11454-6

[14] Lai, J.-Y., & Lin, P.-C. (2024). Real-time surface roughness estimation and automatic regrinding of ground workpieces using a data-driven model and grinding force inputs. *The International Journal of Advanced Manufacturing Technology*, *132*(1), 925–941. https://doi.org/10.1007/s00170-024-13434-w

[15] Maier, M., Rupenyan, A., Bobst, C., & Wegener, K. (2020). Self-optimizing grinding machines using Gaussian process models and constrained Bayesian optimization. *The International Journal of Advanced Manufacturing Technology*, *108*(1), 539–552. https://doi.org/10.1007/s00170-020-05369-9

[16] Liu, K., Chen, Y., Zhang, T., Tian, S., & Zhang, X. (2018). A survey of run-to-run control for batch processes. *ISA Transactions*, *83*, 107–125. https://doi.org/10.1016/j.isatra.2018.09.005

[17] Zhu, T., Cai, M., Gong, Y., Gao, X., Yu, N., & Gong, Q. (2023). Research progress of eco-friendly grinding technology for aviation nickel-based superalloys. *The International Journal of Advanced Manufacturing Technology*, *126*(7), 2863–2886. https://doi.org/10.1007/s00170-023-11336-x

[18] Trishch, R., Petraškevičius, V., Šimelytė, A., Cherniak, O., & Lomanov, K. (2025). Assessment of product quality risks by qualimetric methods using functionally dependent statistics. *Engineering Management in Production and Services*, *17*(3), 65–82. https://doi.org/ 10.2478/emj-2025-0020